Preprints.org

Article

Not peer-reviewed version

Analysis of Transverse Forces for Assessment of Safety against Derailment of the Specialized Train Composition for the Transportation of Long Rails

Valeri Stoilov , Petko Sinapov , Svetoslav Slavchev , Vladislav Maznichki , Sanel Purgic *

Posted Date: 1 December 2023

doi: 10.20944/preprints202312.0008.v1

Keywords: railway; derailment; safety; assessment; long rails transportation; FEM; beam element

Preprints.org is a free multidiscipline platform providing preprint service that is dedicated to making early versions of research outputs permanently available and citable. Preprints posted at Preprints.org appear in Web of Science, Crossref, Google Scholar, Scilit, Europe PMC.

Copyright: This is an open access article distributed under the Creative Commons Attribution License which permits unrestricted use, distribution, and reproduction in any medium, provided the original work is properly cited.

Preprints (www.preprints.org) | NOT PEER-REVIEWED | Posted: 1 December 2023 doi:10.20944/preprints202312.0008.v1

Disclaimer/Publisher's Note: The statements, opinions, and data contained in all publications are solely those of the individual author(s) and contributor(s) and not of MDPI and/or the editor(s). MDPI and/or the editor(s) disclaim responsibility for any injury to people or property resulting from any ideas, methods, instructions, or products referred to in the content.

Article

Analysis of Transverse Forces for Assessment of Safety against Derailment of the Specialized Train Composition for the Transportation of Long Rails

Valeri Stoilov [1], Petko Sinapov [2], Svetoslav Slavchev [1], Vladislav Maznichki [1] and Sanel Purgic [1,*]

[1] Faculty of Transport, Department of Railway Engineering, Technical University Sofia, Sofia 1000, Bulgaria
[2] Faculty of Transport, Department of Mechanics, Technical University Sofia, Sofia 1000, Bulgaria
* Correspondence: s_purgic@tu-sofia.bg; Tel.: +359 898 813 435

Abstract: The study proposes a theoretical method for evaluating the "safety against derailment" indicator of a specialized train composition for the transportation of very long rails. A composition of nine wagons, suitable for the transportation of rails with a length of 120 m, is considered. For the remaining recommended rail lengths, the number of wagons is reduced or increased, the method being modified depending on the required configuration. In accordance with the requirements of EN 14363:2019, the composition is in a curve with a radius of R=150 m. The rails bend, some of them contact the vertical stanchions of the wagon and cause additional transverse forces, which are balanced in the rail track. This is a prerequisite for derailment of the vehicle. The goal of the study is to determine the additional transverse forces that arise because of the bent rails. The task is statically indeterminate, and considering the dimensions of the rails, its solution becomes seriously difficult. For the purposes of the study, the finite element method was used. Based on the displacements of the support points of the rails (caused by the geometry of the curve) the bending line of the elastic load is determined and the forces in the supports are calculated. A group of five rails is considered, with results multiplied proportionally for cases other than five. The resulting forces are considered when determining the derailment safety criterion defined by EN 14363:2019.

Keywords: railway; derailment; safety; assessment; long rails transportation; FEM; beam element

1. Introduction

The European Commission's road map (with a time horizon of 2050) identifies 10 goals in defining transport policy and offers a list of 40 concrete initiatives to achieve the goals. One of them concerns passenger and freight transport, providing:

- reducing the share of road transport, with 50% of all medium-distance transport being carried out by rail and water transport;
- by 2030, 30% of freight transport over 300 km should be carried out by rail or water transport, and by 2050 – over 50%;
- by 2050, most of the passenger transport over more than 300 km should be carried out by rail transport.

The main reasons for the strategic plans formulated in this way are dictated by the huge advantages that rail and water transport have over road and air transport: developed infrastructure, high speed of movement, the possibility of transporting loads of large volume and mass, low cost per unit of work, minimal staff per unit of work, environmental friendliness, high level of safety and others.

In terms of safety (as well as personnel and environmental indicators), rail transport is the undisputed leader among other modes of transport. This stems from the strict regulatory documents for the admission of new vehicles into operation and the regulation of a strict system for operation and maintenance.

© 2023 by the author(s). Distributed under a Creative Commons CC BY license.

Preprints (www.preprints.org) | NOT PEER-REVIEWED | Posted: 1 December 2023 doi:10.20944/preprints202312.0008.v1

A special place for guaranteeing accident-free transport is occupied by the wheel-rail interaction. This is the reason why these elements are the subject of a few current studies [1–4], in which analytical, numerical, and experimental methods related to wheel and rail wear and the derailment phenomenon have been proposed and analyzed. A significant place in modern publications is the elucidation of the derailment mechanism [5–12], in which new factors related to the process are introduced. Their reasons are logical since the phenomenon of derailment is a not infrequent event in the modern reality of railway transport and is associated with serious material damage and casualties. Some of the publications [7,8,10,13–15] investigate specific elements (turnouts, guardrails, switches, track defects, lubricators, crossings) or operational indicators (speed, train length, location of wagons carrying dangerous loads) affecting the wheel-rail system and contributing to the derailment of rolling stock. Many authors [7,8,16] propose the use of numerical methods to theoretically determine the "safety against derailment" indicator. In [17], a new type of finite element for FEM-analysis is proposed, which more accurately reflects the interaction between the wheel and the rail.

The analysis made above clearly shows that there are many theoretically unexplained problems for the occurrence of the derailment process. This is clearly stated in [18], where a critical reading of the currently effective regulatory documents for the admission of new railway vehicles into operation of the European Union, CIS, Great Britain, the USA, China, South Korea, and Japan was made. The authors provide specific explanations of the most common trade-offs, point out the advantages and disadvantages of the methods from the relevant papers, and provide useful recommendations on using simulation methods to assess safety against derailment.

The extensive analysis of available publications allows defining of the following conclusions:

- The derailment phenomenon has a distinctly stochastic character. It depends on many factors, which at a certain moment in a complex combination can lead to its occurrence. Current research addresses the issue of derailment from the point of view of theory enrichment by accounting for one or more additional factors that could influence the occurrence of the adverse event. This effort to clarify the mechanism of the process is undeniably positive for two main reasons: although the wagons commissioned into operation meet the requirements of the regulatory documents, in practice, railway accidents caused by derailments often occur; and second, it could lead to an adjustment of national or international standards, which would reduce the likelihood of derailment.
- Although the proposed criteria are generally valid for the cases of examination of railway vehicles in a loaded or empty state, the safety assessing against derailment is done on an unloaded wagon. The reasons for this are logical - with a full wagon, the vertical force Q increases significantly (especially for freight wagons up to 3-4 times), while the transverse force Y increases less or by the same order under the influence of centrifugal forces.
- Currently, there are regulatory documents that, regardless of their shortcomings, should be respected to reduce the likelihood of derailment.
- In most analyzed publications and in all normative documents related to the derailment process, the evaluation is reduced to the application of Nadal's criterion [18]. The limit value of the ratio (Y/Q) at a coefficient of friction equal 0.36 was determined by Nadal's criterion using Equation (1):

$$\left(\frac{Y}{Q}\right)_{lim} = \frac{\tan\gamma - 0.36}{1 + 0.36\tan\gamma} \quad (1)$$

where γ is the angle of inclination of the wheel flange.

Based on the third conclusion, a theoretical method for evaluating the safety against derailment of a specialized rolling stock for transporting of long rails is proposed in the present study. In this regard, the second conclusion has an important relevance to the problem: when transporting long rails, the load is placed not on one wagon, but on a whole specialized train composition (Figure 1). When passing through a curved section of the track, the elastic rails are deformed and describe a complex curved line, the shape of which depends on the radius of the curve; the number of rails; the type of rails; the method of fixing the rails; the number of vertical columns limiting the transverse displacements inside the gauge of the wagon, etc.

Preprints (www.preprints.org) | NOT PEER-REVIEWED | Posted: 1 December 2023 doi:10.20944/preprints202312.0008.v1

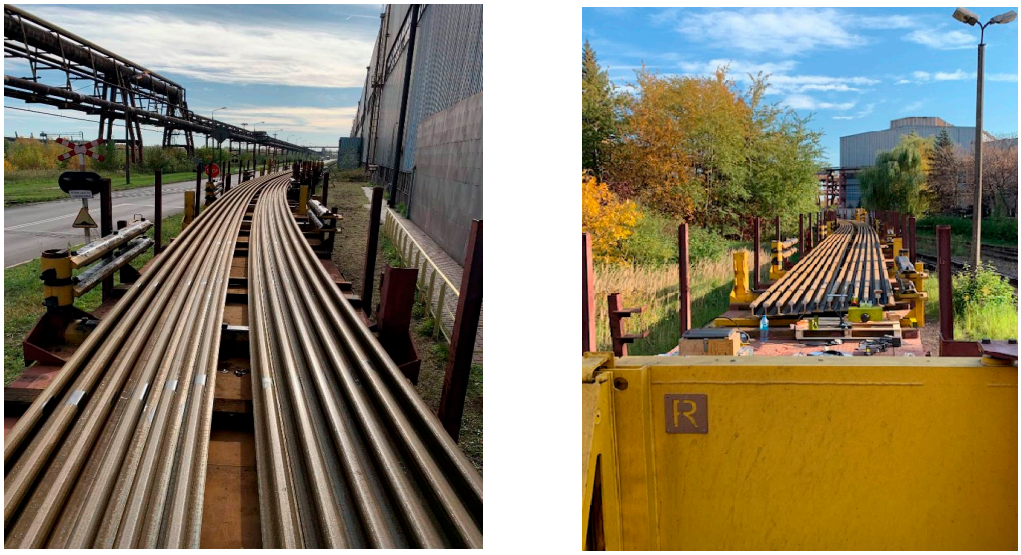

(**a**) (**b**)

Figure 1. Train composition for the transport of long rails in a curve: (**a**) middle view; (**b**) front view (Source: personal archive).

As a result of the interaction of the elastic rails with the vertical columns of the wagon, enormous transverse forces are arising between them, which are transmitted through the vehicle structure and balanced in the rail track. This leads to an increase in the transverse forces Y. The mechanism described above necessitates assessing the safety against derailment not only in a single empty wagon (the case when a new wagon is commissioned into service), but also in the whole train composition, which is loaded to the permissible values.

Based on the above considerations, the study of the safety criterion against derailment should be done through two distinct stages:

- Determination of the transverse forces acting in the central bearings of the bogies, obtained because of the elastic deformations of the transported long rails.
- Application of the method for theoretical assessment of safety against derailment, considering the permissible vertical load and the total values of transverse forces resulting from the movement of the train composition in a curved section of the track and from the elastic deformation of the transported rails.

The first stage takes place in the following sequence, where the steps correspond to the names of Sections 2, 3 and 4 of present paper respectively:

1. development of a computational model for the research object;
2. numerical solution for determining the interaction forces between the deformed rails and the vertical columns of the wagon;
3. determination of the additional forces acting in the central bearings of the bogies.

2. Computational model

The task is complex and complicated, since the dimensions of the studied objects are large, and the deformations are significant. In this case, non-linear effects occur that do not allow obtaining an accurate solution, even when using specialized software. In the literature, there are studies investigating beams where the deformations are large [19–23]. In them, the following task is solved: at a given load, the bending line of the beam is sought. In the present work, the reverse task should be solved: determining the forces that arise at the support points at a given deformation of the investigated beam. For this purpose, a linear analysis method was used, and the research methods from [19–23] can be used to assess the accuracy of the solution.

Preprints (www.preprints.org) | NOT PEER-REVIEWED | Posted: 1 December 2023 doi:10.20944/preprints202312.0008.v1

Basic data and prerequisites for solving the task are:

- In accordance with [24], the train composition is in a curve with radius R=150 m (Figure 2 (a)). The locomotive is not shown in the figure.
- The composition consists of nine wagons, the rails are located on support frames (Figure 2 (b)) and are grouped in separate sections of 5 rails each.
- The middle wagon is equipped with a system to guarantee the immobility of the rails (so called "fixing block") (Figure 2 (b)), and the load/pressure forces are shown in Figure 2 (c).
- On the remaining wagons (not equipped with fixing blocks), three or two (for the end wagons) support frames [25] (Figure 2 (b)) are installed, depending on the length of the transported rails and the number of wagons.
- In the support frames, the rails are placed freely, and unlimited longitudinal displacement is allowed as well as limited transverse displacement within Δh, (Figure 2 (d)). Movements along the vertical direction are limited by the supporting beams of the frames and the clearances Δv (Figure 2 (d)).
- It is assumed that the first four wagons have entered the curve.

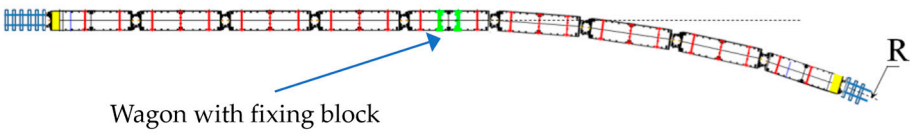

(**a**)

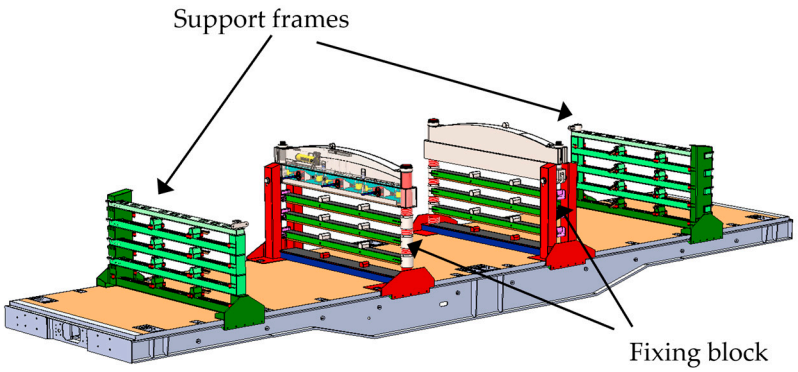

(**b**)

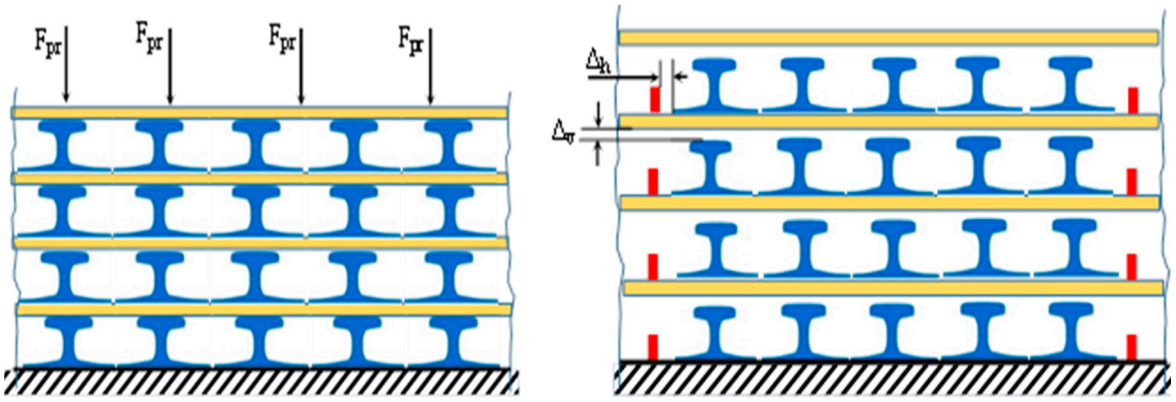

(**c**) (**d**)

Figure 2. Train composition for transportation of long rails: (**a**) Composition in the curve; (**b**) Middle wagon with frames; (**c**) Load/pressure forces in the fixing block; (**d**) Movement limitations in support frames.

Preprints (www.preprints.org) | NOT PEER-REVIEWED | Posted: 1 December 2023 doi:10.20944/preprints202312.0008.v1

The last premise allows only one half of the train composition to be considered (Figure 3). Element A0 defines the position of the fixing block in the middle wagon, and the remaining elements (A1 to A12) define the position of the support frames. The front wagon is equipped with two support frames (A11 and A12) in accordance with the requirements of [25]. The locomotive is not illustrated in Figure 3.

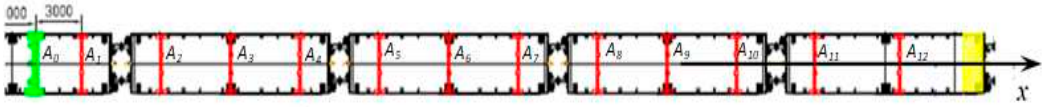

Figure 3. Half of the train composition with elements needed for calculation.

The following additional assumptions were made during the compilation of the computational model:

- The bending of a group of 5 rails (corresponding to one separate section) in the plane *Oxy*, referred to as "group of rails" or "beam" for brevity (Figure 4 and Figure 5);
- Each rail group has a moment of inertia I_{zi} = 0.00000486 m⁴ [26,27]. The total moment of inertia for five rails is $I_z = 5 \cdot I_{zi}$;

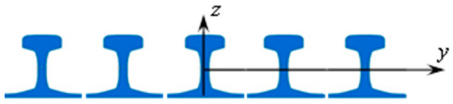

Figure 4. Cross section of one rail group.

- The friction between the rails is neglected due to the peculiarities of the investigated structure.
- In the wagon with the fixing blocks, it is assumed that the rails are immovably fixed, i.e., in the fixing block it is assumed that we have fixed beam (Figure 5 (a));
- At the locations of the supports A_i, it is assumed that unknown forces caused by the deformation of the beam act in the transverse direction (y axis) as shown in Figure 5 (b). The forces are directed perpendicular to the beam axis (x axis);
- Because of the large dimensions and deformations of the system and considering that the task is statically indeterminate, it is solved with a linear analysis method, for the approximate determination of the forces in the supports. The obtained results contain some inaccuracy, which can be estimated by the studies presented in [21,23];
- When moving in a curve with radius *R*=150 m, the speed of the train composition is small, therefore the inertial forces are neglected.

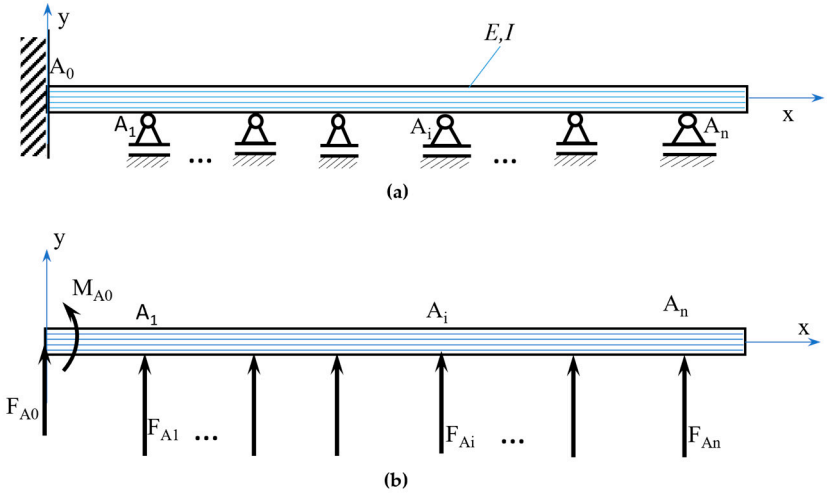

Figure 5. Calculation model of the fixed beam and transverse forces acting on it.

Preprints (www.preprints.org) | NOT PEER-REVIEWED | Posted: 1 December 2023 doi:10.20944/preprints202312.0008.v1

The classical form of the differential equation of the bending line in the given coordinate system and for each section of the beam is given in Equation (2) [28]:

$$\frac{d^2}{dx^2}\left(EI_z\frac{d^2u_y}{dx^2}\right)=q_y \tag{2}$$

For the analytical solution, it is necessary to integrate Equation (2), where a significant number of integration constants appear, depending on the number of sections, which must subsequently be determined by the boundary conditions. For this purpose, the finite element method was applied [28,29]. The presence of the large dimensions of the beams makes it difficult to use precise models like those shown in [1,30,31]. The beam is divided into *n*-number of finite elements, and each of them is located between two adjacent supports A_i (Figure 5). The type of finite element is shown in Figure 6 [28].

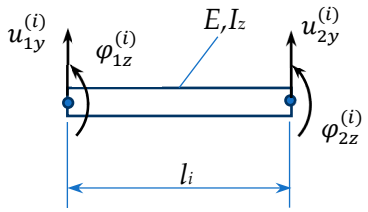

Figure 6. Finite beam element [28].

The position of each element is described by four local coordinates - two displacements and two rotations ($u_{1y}^{(i)},\varphi_{1z}^{(i)},u_{2y}^{(i)},\varphi_{2z}^{(i)}$) of each of the nodes [28].

The stiffness matrix [28,29] of the element *i* is given in Equation (3):

$$[K^{(e)}]=\frac{2EI_z}{l_i^3}\begin{bmatrix}6 & 3l_i & -6 & 3l_i\\ 3l_i & 2l_i^2 & -3l_i & l_i^2\\ -6 & -3l_i & 6 & -3l_i\\ 3l_i & l_i^2 & -3l_i & 2l_i^2\end{bmatrix} \tag{3}$$

where l_i is the length of the element and *E* is the modulus of elasticity.

The discretized model has *n* number of elements (*n*=12 in Figure 7) with different lengths l_i and correspondingly different stiffness matrices. Its position is described by 2*n*+2 global coordinates (Figure 7 (a)). The forces act on the nodes, and the moment acts in node *A*0 (Figure 7 (b)).

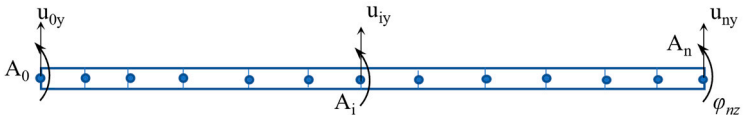

(**a**)

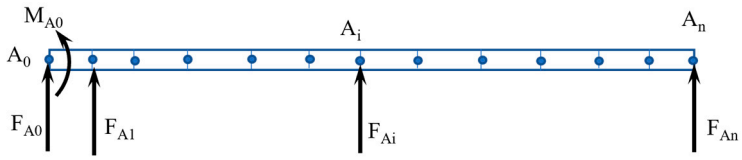

(**b**)

Figure 7. Discretized model of the beam: (**a**) with defined nodes coordinates; (**b**) with defined loads in nodes

Preprints (www.preprints.org) | NOT PEER-REVIEWED | Posted: 1 December 2023 doi:10.20944/preprints202312.0008.v1

For the beam in Figure 7, the Equation (4) is valid:

$$[K_0]\{U_0\}=\{F_0\} \tag{4}$$

where $\{U_0\} = \{u_{0y}, \phi_{0z}, u_{1y}, \phi_{1z}\ldots\ldots, u_{iy}, \phi_{iz}, \ldots\ldots\ldots, u_{ny}, \phi_{nz},\}^T$ is a vector of global coordinates with dimension (2n+2) × 1 and $\{F_0\} = \{F_{A0}, M_{A0}, F_{A1}, 0, F_{A2}, 0\ldots. F_{Ai}, 0..F_{An}, 0\}^T$ is a vector of node loads with dimension (2n+2) × 1. $\{F_0\}$ contains forces and moments applied at the nodes. Except for A0, there are no applied moments in all other nodes. $[K_0]$ is global stiffness matrix, with dimension (2n+2) × (2n+2). Considering that $u_{0y} = 0$ and $\phi_{0z} = 0$ Equation (4) reduces to Equation (5):

$$[K]\{U\}=\{F\} \tag{5}$$

where $[K] = [K_0\ (3{:}2n{+}2, 3{:}2n{+}2)]$ is the stiffness matrix after considering the boundary conditions and has a dimension $2n\times2n$ (the first two rows and columns of the matrix $[K_0]$ are being removed), $\{U\} = \{u_{1y}, \phi_{1z}\ldots\ldots, u_{iy}, \phi_{iz}, \ldots\ldots\ldots, u_{ny}, \phi_{nz},\}^T$ is a vector of global coordinates after considering the boundary conditions and has a dimension $2n\times1$ and $\{F\} = \{F_{A1}, 0, F_{A2}, 0\ldots. F_{Ai}, 0..F_{An}, 0\}^T$ is a vector of node loads after considering the boundary conditions and has a dimension $2n\times1$. F_{A0} and M_{A0} are determined using Equation (6):

$$[K_1]\{U\}=\begin{Bmatrix} F_{A0} \\ M_{A0} \end{Bmatrix} \tag{6}$$

where $[K_1] = [K_0\ (1{:}2, 3{:}2n{+}2)]$ is a $2\times2n$ matrix formed by the first two rows and columns from 3 to $2n$+2 of the matrix $[K]$. In Equation (5) (unlike the classical problem), the displacements u_{iy} are known, but the forces F_{Ai} and rotations φ_{iz} of the nodes are not known. To determine the unknowns, the system is transformed into the form given in Equation (7):

$$[X]\{p\}=\{Z\}\Rightarrow\{p\}=[X]^{-1}\{Z\} \tag{7}$$

In Equation (7), the term $\{p\}$ has a dimension $2n\times1$ and contains the unknowns F_{Ai} and φ_{iz}. It is determined using Equation (8):

$$\{p\}=\left\{F_{A1}, F_{A2}, \ldots F_{An}, \phi_{1z}, \phi_{2z}\ldots\ldots\phi_{nz}\right\}^T \tag{8}$$

The term $\{Z\}$ in equation (7) has a dimension of $2n\times1$ and contains the predetermined displacements u_{iy} of the nodes (coordinates of A_i along the y-axis direction) and elements of the matrix $[K]$. It is determined using Equation (9):

$$\{Z\} = \begin{Bmatrix} K_{1,1}u_{1y} + K_{1,3}u_{2y}\ldots\ldots\ldots + K_{1,2n-1}u_{ny} \\ K_{3,1}u_{1y} + K_{3,3}u_{2y}\ldots\ldots\ldots + K_{3,2n-1}u_{ny} \\ \ldots \\ \ldots\ldots \\ K_{2n-1,1}u_{1y} + K_{2n-1,3}u_{2y}\ldots\ldots\ldots + K_{2n-1,2n-1}u_{ny} \\ K_{2,1}u_{1y} + K_{2,3}u_{2y}\ldots\ldots\ldots + K_{2,2n-1}u_{ny} \\ K_{4,1}u_{1y} + K_{4,3}u_{2y}\ldots\ldots\ldots + K_{4,2n-1}u_{ny} \\ \ldots \\ \ldots\ldots \\ K_{2n,1}u_{1y} + K_{2n,3}u_{2y}\ldots\ldots\ldots + K_{2n,2n-1}u_{ny} \end{Bmatrix} \tag{9}$$

The matrix $[X]$ has a dimension $2n\times2n$, contains the null matrices and the elements of matrix $[K]$. It is determined using Equation (10):

Preprints (www.preprints.org) | NOT PEER-REVIEWED | Posted: 1 December 2023 doi:10.20944/preprints202312.0008.v1

$$[X]=\begin{bmatrix} 1, O_{1,n-1}, -K_{1,2}, -K_{1,4}, -K_{1,6}\ldots\ldots\ldots, -K_{1,2n} \\ 0,1, O_{1,n-2}, -K_{3,2}, -K_{3,4}, -K_{3,6}\ldots\ldots\ldots, -K_{3,2n} \\ \ldots\ldots \\ \ldots \\ O_{1,n-1}, 1, -K_{2n-1,2}, -K_{2n-1,4}, -K_{2n-1,6}\ldots\ldots\ldots, -K_{2n-1,2n} \\ O_{1,n}, -K_{2,2}, -K_{2,4}, -K_{2,6}\ldots\ldots\ldots, -K_{2,2n} \\ O_{1,n}, -K_{4,2}, -K_{4,4}, -K_{4,6}\ldots\ldots\ldots, -K_{4,2n} \\ \ldots \\ \ldots\ldots \\ O_{1,n}, -K_{2n,2}, -K_{2n,4}, -K_{2n,6}\ldots\ldots\ldots, -K_{2n,2n} \end{bmatrix} \quad (10)$$

After determining the unknowns $F_{A1}, F_{A2}, \ldots F_{An}, \phi_{1z}, \phi_{2z}\ldots\ldots\phi_{nz}$ (contained in $\{p\}$), M_{A0} and F_{A0} can be determined from the Equation (6) or from the two equilibrium conditions of the entire beam.

3. Results from the numerical calculations

To determine the coordinates of the points A_i (and the displacements u_{iy} respectively) along the y-axis, it is assumed that the composition is in a curve with radius R (Figure 2 (a)). It is assumed that the points A_1, A_2, A_4, A_5, A_7, A_8, A_{10} and A_{11} lie on the theoretical arc of a circle, because that is where the central bearings of the wagons are positioned. The remaining points A_3, A_6, A_9 and A_{12} are located on the chords between the above points (Figure 3). Their position is determined by the line connecting the central bearings of the wagon. Point A_1 is located at the beginning of the curve.

The coordinate system $A0xy$ is introduced so that the x-axis is in the direction of line A_0-A_1, and its direction relative to the curve is determined by the two central bearings of the wagon with the fixing blocks (Figure 2 (a)). The coordinates of points A_i are given in Table 1.

Table 1. Coordinates of points A_i along the bending line without horizontal clearance between the rails and the support stanchions (Δh=0).

Point	Coordinate x [m]	Coordinate $y=u_{iy}$ [m]
A_0	0	0
A_1	3.000	0
A_2	8.190	-0.168
A_3	12.690	-0.525
A_4	17.190	-0.883
A_5	22.380	-1.540
A_6	26.880	-2.320
A_7	31.380	-3.100
A_8	36.570	-4.241
A_9	41.070	-5.436
A_{10}	45.570	-6.631
A_{11}	50.760	-8.245
A_{12}	56.260	-10.200

The theoretical curve of the bending line, described with the coordinates from Table 1, is shown in Figure 8.

Preprints (www.preprints.org) | NOT PEER-REVIEWED | Posted: 1 December 2023 doi:10.20944/preprints202312.0008.v1

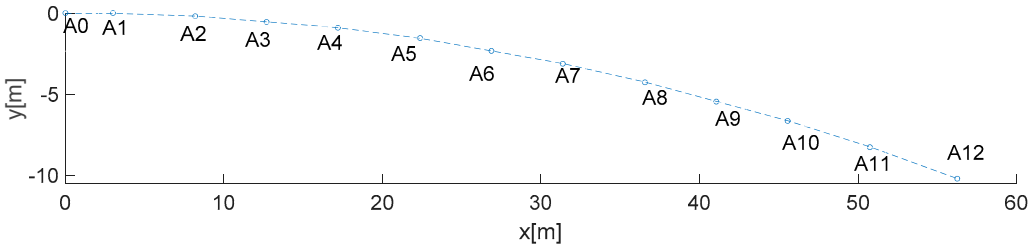

Figure 8. Bending line with coordinates of points A_i.

The determination of the unknown forces F_{Ai} and the moment M_{A0} is carried out in the MATLAB program environment using the displacements from Table 1. Table 2 contains obtained results for force reactions in points A_i. It should be noted that the values are obtained under the condition that there is no horizontal clearance between the rails and the support stanchions, i.e. $\Delta h = 0$ (Figure 2 (d)).

Table 2. Values of reaction forces (and moment M_{A0}) in points A_i without horizontal clearance between the rails and the support stanchions (Δh=0).

Point	Reaction identifier [unit]	Value
A_0	M_{A0} [kNm]	-20.9627
A_0	F_{A0} [kN]	-20.9627
A_1	F_{A1} [kN]	15.4067
A_2	F_{A2} [kN]	28.7388
A_3	F_{A3} [kN]	-45.0839
A_4	F_{A4} [kN]	22.1165
A_5	F_{A5} [kN]	21.0936
A_6	F_{A6} [kN]	-42.6837
A_7	F_{A7} [kN]	21.6934
A_8	F_{A8} [kN]	20.7446
A_9	F_{A9} [kN]	-43.0170
A_{10}	F_{A10} [kN]	25.6134
A_{11}	F_{A11} [kN]	4.9837
A_{12}	F_{A12} [kN]	-8.6432

During the calculations, the presence of large forces was found (Table 2), especially in the points that do not lie on the theoretical arc of a circle (A_3, A_6 and A_9). This is logical and is dictated by the fact that the clearance Δh is not provided in the model, i.e. Δh=0 (Figure 2 (d)). To increase the adequacy of the model, a limited horizontal displacement of the points was allowed due to the available constructively provided clearances between the rails and the support frames. With successive iterations based on a possible displacement of the bending line in the support points, new results for y-coordinates of points A_i were obtained and are presented in Table 3.

Table 3. Adjusted coordinates of points A_i along the bending line with horizontal clearance between the rails and the support stanchions (Δh=90 mm).

Point	Coordinate x [m]	Coordinate $y=u_{iy}$ [m]
A_0	0	0
A_1	3.000	0
A_2	8.190	-0,1436
A_3	12.690	-0,4350
A_4	17.190	-0,8733
A_5	22.380	-1,5400
A_6	26.880	-2,2530
A_7	31.380	-3,1000

Preprints (www.preprints.org) | NOT PEER-REVIEWED | Posted: 1 December 2023 doi:10.20944/preprints202312.0008.v1

A_8	36.570	-4,2410
A_9	41.070	-5,3690
A_{10}	45.570	-6,6274
A_{11}	50.760	-8,2450
A_{12}	56.260	-10,1100

Some of them have been adjusted relative to their original position up to 90 mm (constructively provided clearance between the rails and the support frames) in the transverse direction. In this case, the group of rails does not necessarily rest against each of the side supports, but settles freely, hindered by the minimal frictional forces at the base of the rail. This fact was established during real measurements carried out on a specialized train composition for the transport of long rails. The clearance and possible settlement of the beam at a given point was obtained by iterations through a certain step with a numerical experiment until obtaining the actual measured values. With new coordinates from Table 3, new values of reaction forces are determined and are presented in Table 4.

Table 4. New values of reaction forces (and moment M_{A0}) in points A_i with horizontal clearance between the rails and the support stanchions (Δh=90 mm).

Point	Reaction identifier [unit]	Value
A_0	M_{A0} [kNm]	-21,8257
A_0	F_{A0} [kN]	-21,8257
A_1	F_{A1} [kN]	22,8997
A_2	F_{A2} [kN]	-1,0583
A_3	F_{A3} [kN]	1,3180
A_4	F_{A4} [kN]	-1,0934
A_5	F_{A5} [kN]	-1,1026
A_6	F_{A6} [kN]	1,1627
A_7	F_{A7} [kN]	-0,0952
A_8	F_{A8} [kN]	-0,2744
A_9	F_{A9} [kN]	-0,4341
A_{10}	F_{A10} [kN]	1,2717
A_{11}	F_{A11} [kN]	4,8339
A_{12}	F_{A12} [kN]	-5,6022

4. Determination of the forces acting on the wagons

Analysis of the data from Table 4 shows that the maximum transverse forces are at points A_0 and A_1 of the wagon with fixing block and at points A_{11} and A_{12} of the front (closest to the locomotive) wagon. These forces were used to assess the safety against derailment of the entire specialized train composition. The reason for analyzing the front wagon is that it is at risk of derailment due to the incomplete load with weight from rails (leading to a reduction of the vertical force Q from Equation (1)) and due to the asymmetric distribution of the load in the structure resulting from the placement of the support frames on the wagon (Figure 3).

The forces at points A_0 and A_1 of the wagon with fixing block and at points A_{11} and A_{12} of the front wagon are applied to the wagons (Figures 9 and 10 respectively). The objective is to determine the additional horizontal transverse forces H_{ri} caused by the bent rails and acting on the central bearings of the wagons.

Preprints (www.preprints.org) | NOT PEER-REVIEWED | Posted: 1 December 2023 doi:10.20944/preprints202312.0008.v1

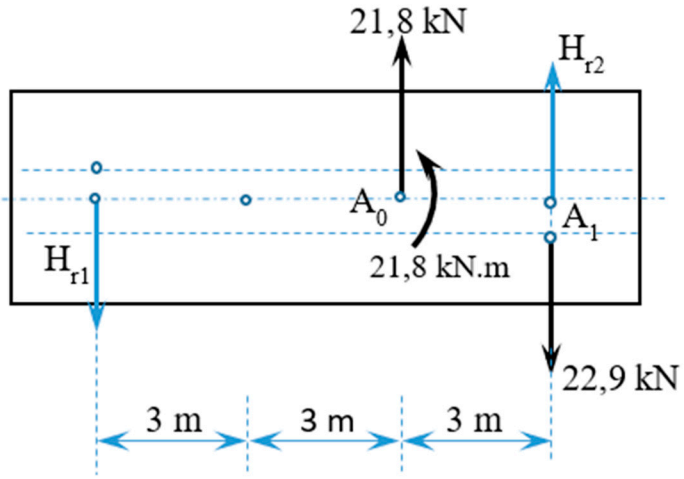

Figure 9. Forces and moment acting on a wagon with fixing block when entering the curve.

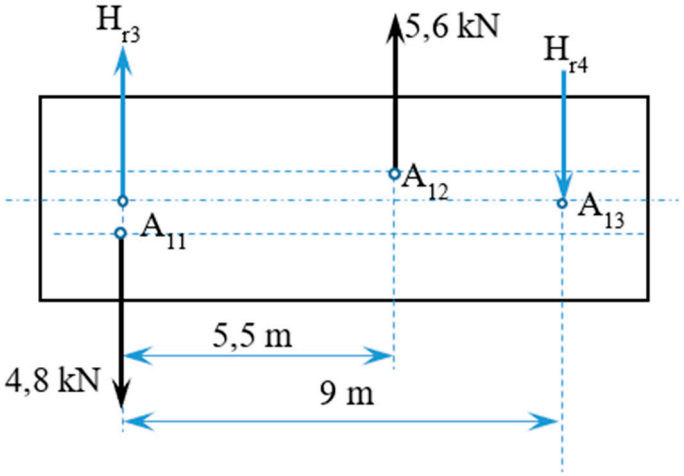

Figure 10. Forces acting on a front wagon.

The determination of the forces H_{ri} is trivial, and their values are:

- For the wagon with the fixing block - H_{r1}=4.84 kN; H_{r2}=5.94 kN;
- For the front wagon - H_{r3}= 2.62 kN; H_{r4}= 3.42 kN;

5. Assessment of safety against derailment

The assessment of safety against derailment of the specialized train composition for transportation of long rails was performed theoretically in full accordance with the method proposed in [32]. Briefly, this is an analytical method developed according to EN 14363:2019 [24], Section 6.1, Method 2 (paragraph 6.1.5.2). The method proposed in [32] has been verified by comparing the results of theoretical and experimental studies and shows a very good compliance.

For assessment purposes, the following corrections were made in the present method compared to [32]:

- The vertical load from the weight of 60 (4 rows x 15 rails per row) rails of type 60E1 with a length of 120 m (on the entire train composition) was applied;
- The horizontal forces from Table 4 are applied in the central bearings of the wagon.

It is assumed that the specialized train composition for transportation of long rails is composed of nine flat wagons of the Smmns series with the following parameters:

Preprints (www.preprints.org) | NOT PEER-REVIEWED | Posted: 1 December 2023 doi:10.20944/preprints202312.0008.v1

- The tare weight of each wagon is 21 tons;
- Distance between pivots is 9 000 mm;
- Maximum load capacity is 69 tons;
- Maximum permissible load capacity when transporting rails is 0.8x69 tons = 49.6 tons according to [25];
- Wagon gauge is G1;
- The weight of two fixing blocks at the middle wagon is 2x2.5 tons = 5 tons;
- The weight of one support frame is 1 ton.

The calculations were performed for a horizontal track without overhang at a friction coefficient $\mu = 0.36$.

Three types of wagons from the loaded train composition were studied:

- The wagon equipped with fixing block to limit the longitudinal movements of the rails during transportation - the reason is that this is the wagon with the maximum tare weight (taking into account the weight of the installed frames) and in it the transverse forces F_{A0} and F_{A1} (Table 4), respectively the transverse forces H_{ni} have a maximum values;
- Front wagon with protective walls. It has a reduced weight of the payload, which is placed asymmetrically on the wagon;
- Intermediate wagon (heaviest loaded wagon of all the wagons discussed above).

Additionally, an assessment was performed also for the empty Smmns series wagon in accordance with the requirements of [24], to assess the influence of the load on the derailment process. Detailed data from the simulation are presented in Table 5 only for the first type of wagon – wagon with fixing block, and for the other types of wagons only the final assessments are given separately in Table 6.

Table 5. Results from calculation of parameters used for assessment of safety against derailment of wagon with fixing block.

Parameter description	Symbol/Equation	Value
Total reaction force of the attacking wheel of wheelset 1	Y_{1a} [1]	122.814 kN
Total reaction force of the non-attacking wheel of wheelset 1	Y_{1i} [1]	-70.732 kN
Minimum deflection of the bogie frame to be reached during tests of the wagon [24]	$\Delta z^{+}_{jk} = g^{+}_{lim} . 2a^{+}$	0.0076 m
Twist of the bogie frame during test ($2a^{+}$ is distance between wheelsets) [24]	$g^{+}_{lim} = 7 - 5/2a^{+}$	4.2222 ‰
Minimum deflection of the wagon frame to be reached during tests of the wagon [24]	$\Delta z^{*} = g^{*}_{lim} . 2a$	33.2 mm
Twist of the wagon frame during test (2a is the pivot distance) [24]	$g^{*}_{lim} = \frac{15}{2a} + 2$	3.6483 ‰
Load force during torsion test	ΔF_p	10 kN
Deflection of the wagon frame under ΔF_p	Δz_p	88.22 mm
Force needed to achieve Δz^{*}	$\Delta F_{z^{*}} = \frac{\Delta F_p . \Delta z^{*}}{\Delta z_p}$	3.763 kN
Maximum force additionally loading bogie frame under $\Delta F_{z^{*}}$	$\Delta F'_{z^{*},max} = \frac{\Delta F_{z^{*}} . (b_{1F} + b_s)}{2b_{1F}}$	3.481 kN
Minimum force additionally loading bogie frame under $\Delta F_{z^{*}}$	$\Delta F'_{z^{*},min} = \Delta F_{z^{*}} - \Delta F'_{z^{*},max}$	0.282 kN
Maximum force overloading first wheel	$\Delta F'_{1z^{*},max} = \frac{\Delta F'_{z^{*},max}}{2}$	1.7405 kN

Preprints (www.preprints.org) | NOT PEER-REVIEWED | Posted: 1 December 2023 doi:10.20944/preprints202312.0008.v1

Minimum force overloading first wheel	$\Delta F'_{1z^*,\min} = \frac{\Delta F'_{z^*,\min}}{2}$	0.141 kN
Additional maximum vertical reaction force in wheels (Equation (25) of [32])	$\Delta Q_{1,\max}$	2.007 kN
Additional minimum vertical reaction force in wheels (Equation (25) of [32])	$\Delta Q_{1,\min}$	-0.125 kN
Nominal vertical force loading the wheels	$Q_{\text{nom}}=Q/N$	93.401 kN
Minimum vertical wheel reaction force	$Q_{\text{jk,min}}= Q_{\text{nom}}+\Delta Q_{1,\min}$	93.276 kN
Minimum vertical wheel reaction force	$Q_{\text{jk,max}}= Q_{\text{nom}}+ \Delta Q_{1,\max}$	95.408 kN

[1] Calculated according to methodology described in [32].

With the data from Table 5 the final assessment of safety against derailment can be conducted. This is performed using Equation (11) and the calculated value is equal to 1.0698. According to [24], when using the theoretical assessment methods, the limit value of 1.2 is reduced by 10%, which means that the limit value of Nadal's criterion should be set to 1.08 and compared with the calculated value, as shown in Equations (12).

$$\left(\frac{Y}{Q}\right)_{ja} = \frac{Y_{ja}}{Q_{jk,\min}+\Delta Q_j}; \qquad \frac{Y_{ja}}{Q_{jk,\min}+\Delta Q_j} \le \left(\frac{Y}{Q}\right)_{\text{lim}} \tag{11}$$

$$\left(\frac{Y}{Q}\right)_{ja} \le \left(\frac{Y}{Q}\right)_{lim}; \qquad 1.0698 \le 1.08 \tag{12}$$

Data for the safety against derailment evaluation criterion for all wagon types considered are given in Table 6.

Table 6. Safety criterion for different wagon types.

Criterion	Wagon with fixing block	Front wagon	Intermediate wagon	Empty wagon
$\left(\frac{Y}{Q}\right)_{ja} \le 1.08$	1.0698	0.8024	0.8295	0.8268

The obtained values of the safety criterion for all wagon types considered are lower than the limit value 1.08 which means that for specialized train composition for transportation of long rails the requirement for safety against derailment is fulfilled.

6. Conclusions

The present study proposes a theoretical method for assessment of safety against derailment of a specialized train composition for the transportation of long rails. For this purpose, a method was developed to determine the horizontal forces in the vertical stanchions of the wagon, occurring when they contact the transported rails in a curved section of the track. The forces are used in the computational model for the study of safety against derailment and an evaluation is made according to Nadal's criterion.

Four different types of train composition wagons were considered: a wagon with fixing blocks, front wagon, intermediate wagon, and an empty wagon. The analysis of the results shows that the wagon with fixing blocks is most at risk of derailment. The obtained value (Table 5) fully corresponds to the requirements of the normative documents not only for real tests (< 1.2), but also for theoretical studies (< 1.08).

The front and intermediate wagons have criterion values very close to that of the empty wagon. This shows that the emerging horizontal elastic forces do not significantly influence the derailment process.

The developed model allows us to evaluate the influence of individual factors like pivot distance, own weight, number of rails, movement speed, overhang of the outer rail of the track,

Preprints (www.preprints.org) | NOT PEER-REVIEWED | Posted: 1 December 2023 doi:10.20944/preprints202312.0008.v1

friction coefficient, etc. on the criterion. It was found that the friction coefficient has the most serious influence. By increasing its value by only one hundredth from 0.36 to 0.37, the criterion increases from 1.0698 to 1.0874 and exceeds the permissible limits for theoretical evaluation.

The remaining parameters relatively less influence the change intensity of the criterion. For example, when reducing the number of rails from 60 (4 rows with 15 rails each) to 45 (3 rows with 15 rails each) as recommended in [25] (the reduction by 25%), the criterion decreases from 1.0698 to 1.0450, i.e., by only 2.37%, which is within the computational error. This makes it inexpedient to use an approach from [25] with only 3 rows of long rails in the composition.

The obtained results show that the transportation of long rails with specialized train composition can be realized on four levels. This will significantly increase the efficiency of operators when delivering long new rails.

The transportation of rails on more than 3 levels is not new in world practice and is widely used in India (a record was set there for the transportation of rails with a length of 260 m, in 5 rows with 12 rails each), the USA, Russia, etc. (in 4 rows with 12-15 rails each).

Author Contributions: Conceptualization, V.S. and P.S.; methodology, V.S. and P.S.; software, S.S., P.S. and V.M.; validation, V.S. and S.P.; formal analysis, P.S., S.S. and V.M.; investigation, P.S. and S.S.; resources, S.S. and S.P.; data curation, S.S. and V.M.; writing—original draft preparation, V.S., P.S. and S.P.; writing—review and editing, V.S., P.S. and S.P.; visualization, S.S. and V.M.; supervision, V.S.; project administration, V.S.; funding acquisition, V.S. All authors have read and agreed to the published version of the manuscript.

Funding: This research was supported by the European Regional Development Fund within the Operational Programme "Science and Education for Smart Growth 2014 - 2020" under the Project CoE "National center of mechatronics and clean technologies" under Grant BG05M2OP001-1.001-0008-C01.

Institutional Review Board Statement: Not applicable.

Informed Consent Statement: Not applicable.

Data Availability Statement: Data is contained within this article.

Acknowledgments: The authors would like to thank the Research and Development Sector at the Technical University of Sofia for the financial and technical support.

Conflicts of Interest: The authors declare no conflict of interest.

References

1. Jagadeep, B.; Kumar, P.-K.; Subbaiah, K.-V. Stress Analysis on Rail Wheel Contact. *Int. J. Res. Eng.* **2018**, *1(5)*, 47-52.
2. Bosso, N.; Magelli, M.; Zampieri, N. Simulation of wheel and rail profile wear: a review of numerical models. *Rail. Eng. Sci.* **2022**, *30(4)*, 403-436.
3. Gao, Y.; Wang, P.; Wang, K. et al. Damage tolerance of fractured rails on continuous welded rail track for high-speed railways. *Rail. Eng. Sci.* **2021**, *29*, 59–73.
4. Milković, D.; Simić, G.; Radulović, S.; Lučanin, V.; Kostić, A. Experimental approach to assessment of safety against derailment of freight wagons, In *Experimental Research and Numerical Simulation in Applied Sciences. CNNTech* 2022; Lecture Notes in Networks and Systems, 564; Mitrovic, N., Mladenovic, G., Mitrovic, A., Eds.; Springer, Cham, Switzerland, 2023.
5. Zeng, J.; Wu, P. Study on the wheel/rail interaction and derailment safety. *Wear*, **2008**, *265*, 1452–1459.
6. Matsumoto, A.; Michitsuji, Y.; Ichiyanagi, Y.; Sato, Y.; Ohno, H.; Tanimoto, M.; Iwamoto, A.; Nakai, T. Safety measures against flange-climb derailment in sharp curve-considering friction coefficient between wheel and rail, *Wear*, **2019**, *432-433*, 202931.
7. Lai, J. et al., Investigation on train dynamic derailment in railway turnouts caused by track failure, *Eng. Fail. Anal.*, **2022**, *134*, 106050.
8. Yang, Z.; Li, Z. Wheel-rail dynamic interaction. In *Woodhead Publishing Series in Civil and Structural Engineering - Rail Infrastructure Resilience*, 111-135, Calçada, R., Kaewunruen, S., Eds.; Woodhead Publishing: Cambridge, UK, 2022.
9. Huang, J.-Y. Nadal's Limit (L/V) to Wheel Climb and Two Derailment Modes. *Eng. Phys.* **2021**, *5*, 8-14.
10. Atmadzhova, D. Analysis of mathematical expressions for determine the criteria derailment of railway wheelset. *Mech. Transp. Comm.* **2011**, *3*, 42-49.

Preprints (www.preprints.org) | NOT PEER-REVIEWED | Posted: 1 December 2023 doi:10.20944/preprints202312.0008.v1

11. Song, I.-H.; Koo, J.-S.; Shim, J.-S.; Bae, H.-U.; Lim, N.-H. Theoretical Prediction of Impact Force Acting on Derailment Containment Provisions (DCPs). *Appl. Sci.* **2023**, *13*, 3899.
12. Santamaria, J.; Vadillo, E.-G.; Gomez, J. Influence of creep forces on the risk of derailment of railway vehicles, *Veh. Syst. Dyn.* **2009,** *47*, 721-752.
13. Ishida, M.; Ban, T.; Iida, K.; Ishida, H.; Aoki, F. Effect of moderating friction of wheel/rail interface on vehicle/track dynamic behaviour. *Wear*, **2008**, *265*, 1497-1503.
14. Sala, A.J.; Felez, J.; de Dios Sanz, J.; Gonzalez, J. New Anti-Derailment System in Railway Crossings. *Machines* **2022**, *10*, 1224.
15. Anderson, R.-T.; Barkan, C.-P.-L. Derailment Probability Analyses and Modeling of Mainline Freight Trains. In Proceedings of the 8th International Heavy Haul Conference, 491-497, Rio de Janeiro, Brazil, 14-16 June 2005.
16. Kalivoda, J.; Neduzha, L. Simulation of Safety Against Derailment Tests of an Electric Locomotive. In Proceedings of 25th International Conference Engineering Mechanics, 177–180, Svratka, Czech Republic, 13–16 May 2019.
17. Ju, S.-H.; Ro, T.-I. Vibration and Derailment Analyses of Trains Moving on Curved and Cant Rails. *Appl. Sci.* **2021**, *11*, 5106.
18. Wilson, N.; Fries, R.; Wittea, M.; Haigermoser, A.; Wrang, M.; Evans, J.; Orlova, A. Assessment of safety against derailment using simulations and vehicle acceptance tests: A worldwide comparison of state-of-the-art assessment methods. *Veh. Syst. Dyn.* **2011**, *49,* 1113-1157.
19. Shvartsman, B.-S. Direct method for analysis of flexible cantilever beam subjected to two follower forces. *Int. J. Non.-Lin. Mech.* **2009**, *44,* 249-252.
20. Ghuku, S.; Saha K.-N. A theoretical and experimental study on geometric nonlinearity of initially curved cantilever beams. *Eng. Sci. Tech. Int. J.* **2016**, *19*, 135-146.
21. Beléndez, T.; Neipp, C.; Beléndez, A. Large and small deflections of a cantilever beam. *Eur. J. Phys.* **2002**, *23*, 371-379.
22. Kocatürk, T.; Akbaş, Ş.-D.; Şimşek, M. Large deflection static analysis of a cantilever beam subjected to a point load. *Int. J. Eng. Appl. Sci.* **2010**, *2*, 1-13.
23. Wang, C.-M.; Lam, K.-Y.; He, X.-Q.; Chucheepsakul, S. Large deflections of an end supported beam subjected to a point load. *Int. J. Non.-Lin. Mech.* **1997**, *32,* 63-72.
24. *EN 14363:2019*; Railway applications – Testing and Simulation for the acceptance of running characteristics of railway vehicles – Running Behaviour and stationary tests. European Committee for Standardization: Brussels, Belgium, 2019.
25. Loading Guidelines. Code of practice for the loading and securing of goods on railway wagons. Volume 2. Goods. 7th Edition. International Union of Railways (UIC): Paris, France, 2023.
26. *EN 13674-1:2011*; Railway applications - Track - Rail - Part 1: Vignole railway rails 46 kg/m and above. European Committee for Standardization: Brussels, Belgium, 2011.
27. Specifications Of UIC 60 Steel Rail. Available online: https://www.railroadpart.com/news/specifications-of-uic-60-steel-rail.html (accessed on 16th November 2023).
28. Merkel, M.; Öchsner, A. *Eindimensionale Finite Elemente*, 2nd ed.; Springer-Verlag: Berlin Heidelberg, Germany, 2015; pp. 79–83.
29. Rao, S.-S. *The Finite Element Method in Engineering*, 5th ed.; Butterworth-Heinemann: Oxford, UK, 2011; pp. 311-354.
30. Gardie, E.; Dubale, H.; Tefera, E.; Bezzie, Y.-M.; Amsalu, C. Numerical analysis of rail joint in a vertical applied load and determining the possible location of joints. *Forc. Mech.* **2022**, *6*, 100064.
31. Kukulski, J.; Jacyna, M.; Gołębiowski, P. Finite Element Method in Assessing Strength Properties of a Railway Surface and Its Elements. *Symmetry* **2019**, *11*, 1014.
32. Stoilov, V.; Slavchev, S.; Maznichki, V.; Purgic, S. Method for Theoretical Assessment of Safety against Derailment of New Freight Wagons. *Appl. Sci.* **2023**, *13*, 12698.

Disclaimer/Publisher's Note: The statements, opinions and data contained in all publications are solely those of the individual author(s) and contributor(s) and not of MDPI and/or the editor(s). MDPI and/or the editor(s) disclaim responsibility for any injury to people or property resulting from any ideas, methods, instructions or products referred to in the content.